Vimentin-Dependent Spatial Translocation of an Activated MAP Kinase in Injured Nerve

Eran Perlson,[1] Shlomit Hanz,[1] Keren Ben-Yaakov,[1]
Yael Segal-Ruder,[1] Rony Seger,[2]
and Mike Fainzilber[1,*]
[1]Department of Biological Chemistry
[2]Department of Biological Regulation
Weizmann Institute of Science
76100 Rehovot
Israel

Summary

How are phosphorylated kinases transported over long intracellular distances, such as in the case of axon to cell body signaling after nerve injury? Here, we show that the MAP kinases Erk1 and Erk2 are phosphorylated in sciatic nerve axoplasm upon nerve injury, concomitantly with the production of soluble forms of the intermediate filament vimentin by local translation and calpain cleavage in axoplasm. Vimentin binds phosphorylated Erks (pErk), thus linking pErk to the dynein retrograde motor via direct binding of vimentin to importin β. Injury-induced Elk1 activation and neuronal regeneration are inhibited or delayed in dorsal root ganglion neurons from _vimentin_ null mice, and in rats treated with a MEK inhibitor or with a peptide that prevents pErk-vimentin binding. Thus, soluble vimentin enables spatial translocation of pErk by importins and dynein in lesioned nerve.

Introduction

How are kinase signals propagated over long distances within a cell? This fundamental question in cell biology is especially acute in the case of neurons, which are highly polarized and differentiated cells with axonal and dendritic processes that extend over distances of millimeters to meters in large mammals. Local generation of signal in an axon or dendrite by phosphorylation of a signaling kinase must be followed in many cases by propagation of the signal back to the cell body and the nucleus. Quantitative theoretical analyses have shown that under typical protein diffusion rates and cytosolic phosphatase activity levels, activated MAP kinases should be dephosphorylated to basal levels within a few microns of the site of activation (Kholodenko, 2003), unless the signal is protected or regenerated en route. A number of possibilities have been suggested, including lateral propagation from kinase to kinase at the cell surface (Reynolds et al., 2003), formation of multivesicular bodies that package the phosphorylated kinase (Weible and Hendry, 2004), or generation of signaling endosomes containing both ligand and receptor (Howe and Mobley, 2004). Despite this diversity of potential mechanisms for membrane-associated signals, to date there is no experimental data demonstrating how a kinase signal might be transported over long in-

tracellular distances in nonvesiculated signaling complexes.

Retrograde injury-signaling mechanisms in lesioned nerve provide an intriguing example of a nonvesiculated long-distance signaling complex. Mammalian peripheral and invertebrate central nerves are capable of functional regeneration, in part due to intrinsic mechanisms activated in the neuronal cell body (Goldberg, 2003). The cell body response can be triggered or enhanced by protein injury signals retrogradely transported from lesion sites (Perlson et al., 2004a). We have recently shown that injury-induced regulation of importins in axons provides a mechanism for retrograde signaling after lesion, due to a constitutive interaction of importin α with dynein. The signaling is thought to depend on endogenous regeneration-modulating proteins that utilize the nuclear localization signal (NLS) binding site of the importins for retrograde transport (Hanz et al., 2003).

The precise identity of the NLS-bearing retrograde signals is still unknown, but others have implicated a MAP kinase Erk1/2 homolog in retrograde injury signaling in _Aplysia_ neurons (Sung et al., 2001). Nuclear import of most Erk family members is not dependent on classical NLS binding to importin α/β heterodimers (Whitehurst et al., 2002). Do activated MAP kinases access the same retrograde injury-signaling mechanism? We used differential proteomics as a nonbiased method to seek out components of the system and identified soluble cleavage products of an intermediate filament (IF) protein as a major component of the retrograde protein ensemble after nerve lesion in a mollusk (Perlson et al., 2004b). Truncation mutants of the closely related mammalian type III IF vimentin can translocate from cytoplasm to nucleus in transfected cells (Rogers et al., 1995). Moreover, vimentin is known to interact with signaling molecules (Paramio and Jorcano, 2002). We therefore examined potential roles of mammalian type III intermediate filaments in retrograde injury signaling in the sciatic nerve and in neurons of the dorsal root ganglia (DRG). Here, we show that vimentin expression is elevated in sciatic nerve axoplasm after injury. Vimentin links pErk to importin β in the retrograde injury-signaling complex and enables retrograde transport of activated MAP kinases in sensory axons.

Results

The molluscan IF identified in our proteomics screen was found to be most homologous to the vertebrate type III IF _vimentin_ (Figure 1A). In the nervous system, _vimentin_ is most prominently expressed in glial cells (Menet et al., 2003), but it is also expressed in neurons early in development and following injury, where it has been suggested to play a role in early generation and extension of neurites (Boyne et al., 1996; Dubey et al., 2004). _peripherin_ is another closely related type III IF that is highly expressed in peripheral nerve axons and upregulated by injury (Lariviere and Julien, 2004). We

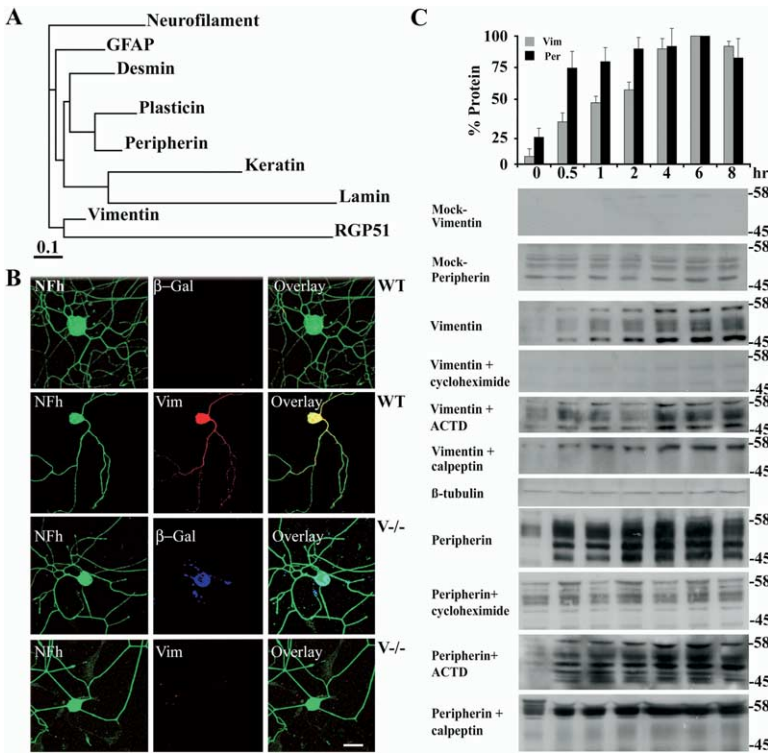*Correspondence: mike.fainzilber@weizmann.ac.il

Figure 1. Vimentin and Peripherin Are Upregulated in Axoplasm after Nerve Injury

(A) A phylogenetic tree constructed using ClustalX reveals the evolutionary relatedness of vertebrate vimentin and other type III intermediate filaments to the *Lymnaea* intermediate filament RGP51.

(B) Immunostaining of adult wild-type and *vimentin*⁻/⁻ DRG neurons after 2 days in culture reveals expression of vimentin (red) in the wild-type but not in the *vimentin*⁻/⁻ neurons, and β-gal (blue) in *vimentin*⁻/⁻ but not in wild-type. Colocalization with the axonal marker NFH (green) showed vimentin expression in both cell body and neurites. Cell counts revealed that 64% of the wild-type NFH-positive neurons expressed vimentin, while 58% of the *vimentin*⁻/⁻ neurons expressed β-gal. Scale bar, 20 μm.

(C) Western blot analysis of postlesion axoplasm reveals upregulation of vimentin and peripherin. Adult rats were anesthetized and subjected to sciatic nerve crush, and axoplasm was obtained from nerves dissected at the indicated times postlesion. Aliquots (40 μg) of axoplasm were analyzed by Western blot and quantified in reference to the level of vimentin and peripherin at 6 hr. Calpeptin (100 μM), cycloheximide (10 μg/ml), or actinomycin-D (5 μg/ml) was applied to the nerve by injection concomitantly with the injury. β-tubulin was used to confirm equal loading. The quantification is in percent of protein levels at 6 hr postlesion (averages ± standard deviation; n = 3).

examined the expression of vimentin or peripherin in the sciatic nerve and DRG and observed vimentin immunostaining in the cell body and processes of approximately 60% of adult wild-type NFH-positive sensory neurons in culture (Figure 1B). A corresponding fraction of *vimentin* null neurons stained positively for β-galactosidase (β-gal), thus confirming expression of the *vimentin* locus after lesion. We then examined occurrence of both IFs in sciatic nerve axoplasm in vivo, after verifying purity of the axoplasm preparations by lack of immunoreactivity for S100 and RCC1 (data not shown), as well as lack of other glial or nuclear markers (see Figure S1 in the Supplemental Data available with this article online). Little or no IF was found in axoplasm before injury, but within 30 min of a lesion we observed the appearance of soluble forms of both vimentin and peripherin (Figure 1C). Levels of these proteins increased during 8 hr following injury, and it was possible to block the increase by injecting the nerve with cycloheximide (CHX), an inhibitor of translation, but not with actinomycin-D (ACTD), an inhibitor of transcription. The lower molecular masses of both IFs were lost upon treatment of the nerve with the calpain inhibitor calpeptin. Addition of calpeptin to already extracted axoplasm had no effect on the vimentin pattern observed (data not shown). Thus, soluble forms of vimentin and peripherin are produced in injured sciatic nerve axoplasm by a combination of local translation and calpain cleavage activity.

We then examined coimmunoprecipitation of vimentin or peripherin with the dynein motor complex in injured nerve. Vimentin was observed to coprecipitate with dynein in increasing amounts with time after injury (Figure 2A). In contrast, peripherin was not found in any of the precipitates, despite the high levels of peripherin found in axoplasm at these time points (see Figure 1C). The increased amounts of vimentin coprecipitating with dynein over time after injury are a direct consequence of the increasing amounts of vimentin and importin β, since analyses of precipitated over input levels revealed similar pull-down efficiency at the different time points (data not shown). As reported previously, importin α4 was found in the complex in both uninjured and lesioned nerve, while importin β levels increased in the coprecipitate after injury (Figure 2A). Reciprocal coimmunoprecipitations with an antibody directed against vimentin revealed increasing amounts of dynein, importin α, and importin β with time after injury (Figure 2B). Does vimentin access the NLS binding site in the complex? We addressed this issue by conducting coprecipitation experiments of dynein with vimentin in the presence of excess NLS peptide or reverse-NLS peptide as control. As shown in Figure 2C, the interaction of vimentin with dynein is not competed by excess NLS. Silver staining of 2D-PAGE from such pull-downs revealed other protein spots that are displaced from the dynein complex by NLS peptide (data not shown). Moreover, vimentin coprecipitates from axoplasm together with the importins in NLS pull-downs (Figure 2D), indicating that a vimentin-importin interaction cannot be mediated via the NLS binding site. A number of nonclassical importin cargoes undergo nuclear uptake
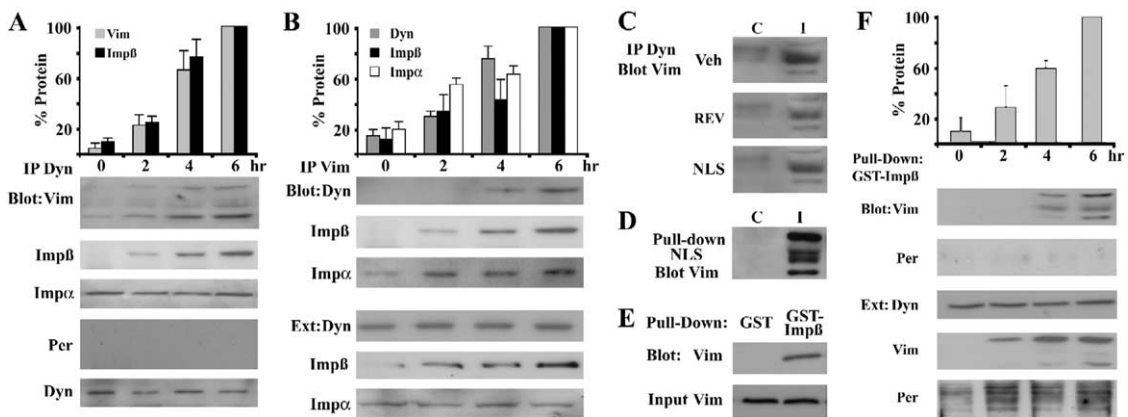
Figure 2. Vimentin Interacts with the Dynein/Importin Complex after Nerve Injury

(A) Vimentin, importin β, and importin α but not peripherin were coprecipitated with dynein from axoplasm (500 μg input per lane) at 0–6 hr postlesion. (B) Dynein, importin β, and importin α were coprecipitated with vimentin at the indicated times postlesion. Quantification in both (A) and (B) is in reference to protein levels at 6 hr postlesion (averages ± standard deviation; n = 3). (C) Coprecipitation of vimentin with dynein was not affected by coincubation with NLS or reverse-NLS (REV) peptides at 2 μM concentration. "C," axoplasm from control nerve; "I," axoplasm from injured nerve 6 hr postlesion. (D) Vimentin coprecipitates in an NLS pull-down assay. Biotinylated NLS peptide (30 μg) was injected to sciatic nerve before extraction of axoplasm, and an additional 5 μg peptide was added to 0.5 mg axoplasm protein and incubated for 1 hr at room temperature, followed by pull-down on streptavidin dynabeads. Proteins were eluted with 0.1% TFA and subjected to Western blot analysis. (E) Direct interaction of importin β and vimentin in vitro. GST-importin β (1 μg) was incubated with vimentin (0.1 μg) for 2 hr at 37°C before GST pull-down. GST alone was used as a negative control. The experiments in (C)–(E) were each repeated at least three times with similar results. (F) GST-importin β (1 μg) was incubated with axoplasm (500 μg) from 0–6 hr postlesion for 2 hr at 37°C. The pull-down revealed coprecipitation of vimentin but not peripherin. Quantification of pulled-down vimentin is shown in reference to protein levels at 6 hr postlesion (averages ± standard deviation; n = 3).

by direct binding to importin β (Harel and Forbes, 2004). We therefore tested for a direct interaction of vimentin with importin β by in vitro coprecipitation of vimentin with a GST-importin β fusion protein. Purified recombinant vimentin was readily pulled down with GST-importin β but did not precipitate with GST alone (Figure 2E). Finally, GST-importin β was incubated with axoplasm from different times after lesion, and Western blots of pull-downs were probed for both vimentin and peripherin. As shown in Figure 2F, increasing amounts of vimentin were found in the pull-downs in correlation with time after lesion, whereas peripherin could not be detected at any of the time points examined.

Having established that soluble forms of vimentin interact with the importin-dynein retrograde complex after nerve injury, we wished to determine the role of this intermediate filament molecule in the complex. Vimentin has been suggested to act as a scaffold or carrier for signaling molecules (Paramio and Jorcano, 2002) or to directly modulate nuclear architecture and/or transcription (Traub and Shoeman, 1994). The *Aplysia* data implicating Erk-like kinases in retrograde injury signaling (Sung et al., 2001) suggested that vimentin might act as a scaffold for the retrograde transport of Erks in mammalian nerve. We therefore examined the activation of MAP kinases in lesioned rat sciatic nerve and observed phosphorylation of axoplasmic Erk1/2 within 30 min and lasting at least 8 hr after injury (Figure 3A). Immunoprecipitation of either vimentin or dynein from axoplasm revealed coprecipitation of pErk increasing with time after lesion (Figure 3B). Incubation of recombinant GST-pErk2 with axoplasm from different time points after lesion revealed coprecipitation of increas-

ing amounts of vimentin but not peripherin (Figure 3C). We then examined retrograde transport of vimentin and pErk after sciatic nerve lesion in vivo. Crushed nerves from adult rats at increasing times after lesion were divided into consecutive segments as shown in Figure 4A. Axoplasm from each segment was subjected to dynein immunoprecipitation, and precipitates were then analyzed by Western blot for presence of vimentin and pErk. Both molecules moved retrogradely together with dynein over the time course of the experiment, arriving at the L4/L5 DRGs approximately 20 hr after the lesion. Interestingly, vimentin remained associated with dynein up to the 24 hr time point in the DRG, whereas the pErk was not found in the complex shortly after arrival in the ganglia (Figure 4A), thus potentially freeing the MAP kinase for interaction with cytoplasmic or nuclear substrates in the cell body. Erks modulate gene expression by directly phosphorylating transcription factors such as the ETS domain factor Elk1. We therefore examined the time course of Elk1 phosphorylation in L4/L5 DRG after sciatic nerve lesion in adult rats. Two peaks of Elk1 phosphorylation were observed in DRG lysates: an initial, very rapid event that may be in response to membrane depolarization caused by the crush and a second, more sustained phosphorylation that commences upon arrival of pErk in the ganglia (Figure 4B). We verified that the later phosphorylation event indeed occurs in neurons by immunostaining of L4/L5 ganglion sections for NFH and pElk1. As shown in the right panel of Figure 4B, phosphorylated Elk1 is concentrated in nuclei of NFH-positive neuronal cell bodies 24 hr after sciatic nerve lesion.

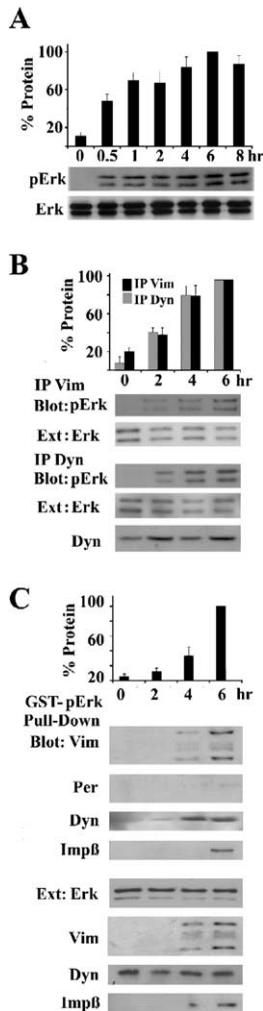The discrepancy between dissociation times of vi-

Figure 3. Vimentin Interacts with pErk in Lesioned Nerve

(A) Western blot analysis of 40 μg aliquots of axoplasm from 0 to 8 hr postlesion reveals phosphorylation of Erk1 and Erk2 after injury. Reprobing of the blot with a general Erk antibody was used to control for equal loading. Quantification is in percentage of pErk levels at 6 hr postlesion (average ± standard deviation; n = 3).

(B) Immunoprecipitation of dynein or vimentin from 500 μg axoplasm taken at 0–6 hr postlesion shows an increase in coprecipitating pErk levels with time. The quantification is in reference to coprecipitating pErk levels at 6 hr postlesion (average ± standard deviation; n = 3). General Erk and dynein were used as loading controls (40 μg protein per lane).

(C) GST-pErk pull-down from axoplasm 0–6 hr postlesion reveals coprecipitation of vimentin but not peripherin. The quantification shows coprecipitating vimentin as percent of maximum (averages ± standard deviation; n = 3). The GST-pErk (0.5 μg) was incubated with 500 μg of axoplasm protein obtained at the indicated postlesion times. General Erk and dynein were used as loading controls, and axoplasm levels of vimentin and importin β are also shown for comparison (40 μg axoplasm protein per lane).

Figure 4. Retrograde Transport of Vimentin and pErk

(A) Coimmunoprecipitation of vimentin and pErk with dynein from 300 μg aliquots of axoplasm obtained from lesioned sciatic nerve segments I–III and DRG extract IV as indicated in the schematic. I indicates the segment adjacent to the lesion site. The DRG extraction (IV) was in lysis buffer. Sampling at 0–24 hr postlesion revealed retrograde movement of both pErk and vimentin with dynein until arrival in the DRG at 20 hr postlesion. At the 24 hr time point, only vimentin was still found in association with dynein in the DRG. Dynein was used as a loading control for all lanes in the time series. Graphs to the right of each set of gels quantify the corresponding distribution of dynein-associated vimentin and pErk along the nerve as percent of maximum (average ± standard deviation; n = 4).

(B) Phosphorylation of Elk1 in L4/L5 DRGs from the experiment of (A). (Left) Aliquots (50 μg) of DRG lysates from the indicated postlesion times (hr) were analyzed by Western blot for pElk1. General Erk was used as the loading control (50 μg total protein per lane). (Right) Immunostaining of a DRG cross-section 24 hr postlesion for the neuronal marker NFH (green) and pElk1 (red). Scale bar, 50 μm. Repeated three times with similar results.

mentin and pErk from the dynein complex upon arrival at the ganglia suggested differential regulation of these two interactions. Nerve injury is known to cause a significant increase in intracellular calcium levels in axons (Mandolesi et al., 2004). We therefore tested the effects of calcium on the pErk-vimentin and vimentin-importin
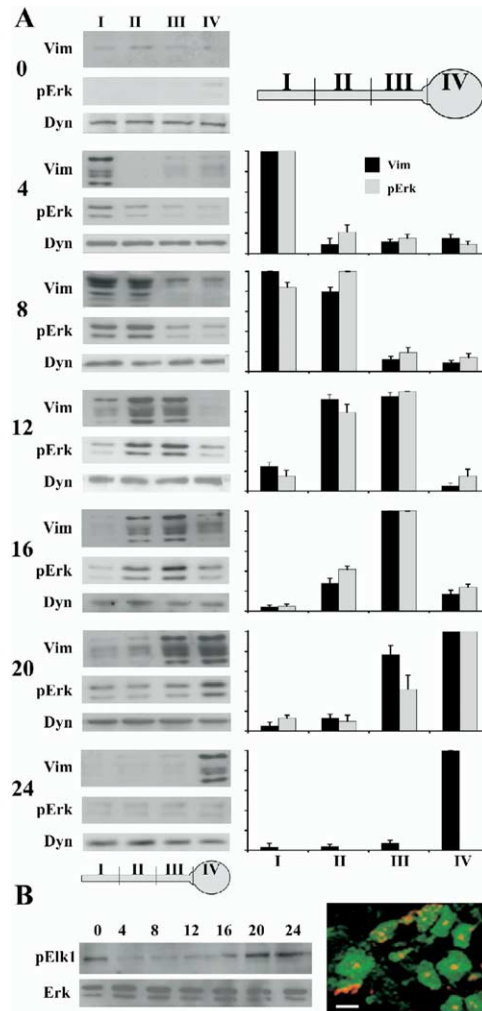
interactions and found that vimentin binding to pErk2 in vitro was calcium dependent, increasing at calcium concentrations of up to 1 μM (Figure 5A). In contrast, changing calcium concentrations had little or no effect on the vimentin-importin β interaction. Similar experiments with nonphosphorylated Erk2 revealed that bind-
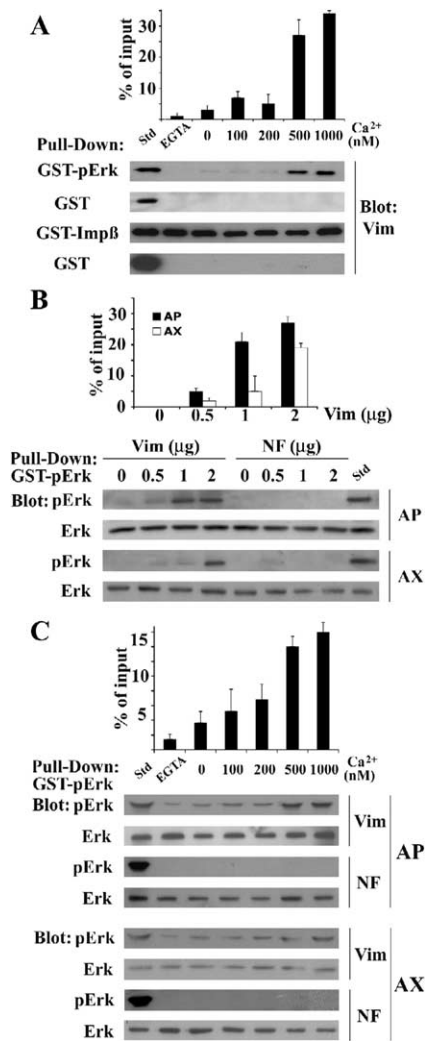
Figure 5. Effects of Calcium on Vimentin-pErk Binding and Erk Phosphorylation

(A) GST-pErk (0.5 μg) or GST-importin β (1 μg) was incubated with vimentin (0.1 μg) in NTB with the indicated calcium concentrations or with 2 mM EGTA for 2 hr at 37°C. GST alone was used as negative control. The gel standard (Std) is 50 ng vimentin. Quantification is shown as percent of input vimentin (average ± standard deviation; n = 3).

(B) Concentration-dependent phosphatase protection of pErk by vimentin. Importin β (2 μg) was incubated with GST-pErk (0.1 μg) and with the indicated amounts (μg) of vimentin or neurofilament (NF) for 2 hr in NTB containing 1 μM calcium at 37°C. Alkaline phosphatase (AP; 2 U) or axoplasm from injured nerve 6 hr postlesion (AX; 100 μg) was added for an additional 30 min before performing GST pull-down followed by Western blotting for pErk. Vimentin protected pErk from dephosphorylation in a concentration-dependent manner. The gel standard (Std) is 20 ng GST-pErk. Quantification is shown as percent of input pErk (average ± standard deviation; n = 3).

(C) Phosphatase protection of pErk by vimentin is calcium dependent. The experiment was carried out as described in (B) at a single concentration (2 μg) of vimentin or NF and at the indicated concentrations of calcium or 2 mM EGTA. Note that calcium dependence of the phosphatase protection parallels the calcium dependence of vimentin-pErk binding shown in (A).

ing of nonphosphorylated Erk to vimentin is reduced at high calcium concentrations (data not shown). Therefore, another possible explanation for the apparent dissociation of pErk in the cell body might be dephosphorylation of the kinase. We examined this issue by testing the effects of increasing concentrations of vimentin on Erk phosphorylation in the presence of alkaline phosphatases (APs) or of sciatic nerve axoplasm. Strikingly, vimentin levels in the range of 3-fold to 6-fold molar ratio of vimentin to pErk provided almost complete in vitro protection of pErk2 from the phosphatases, while similar levels of neurofilament (NF) had no effect (Figure 5B). The protection of pErk by vimentin was specific, as identical concentrations of vimentin had no effect on hydrolysis of p-nitrophenyl phosphate (pNPP) by AP (data not shown). The calcium dependence of pErk binding to vimentin prompted us to examine if the in vitro phosphatase protection provided by vimentin could also be modulated by calcium. As shown in Figure 5C, vimentin protected pErk2 from dephosphorylation in vitro in a calcium-dependent manner, and in the same range of calcium concentrations that support pErk-vimentin binding.

The data described thus far indicate that soluble forms of vimentin interact with the importin-dynein retrograde complex in injured rat sciatic nerve and thereby enable transportation of pErk from the lesion site to activate substrates such as Elk1 in neuronal cell bodies. We tested these findings by comparing immunoprecipitates of dynein from sciatic nerve axoplasm of wild-type and *vimentin*^{-/-} mice. The pErks coprecipitated with dynein in injury axoplasm from wild-type mice but not from *vimentin* nulls (Figure 6A). Injury-induced Erk phosphorylation was similar in wild-type and *vimentin*^{-/-} axoplasm; thus, the specific difference was the lack of interaction of pErk with the dynein complex in *vimentin* null animals. We then examined retrograde accumulation of p-Erk in a lesion-ligation paradigm in sciatic nerves of wild-type versus *vimentin* null mice. As shown in Figure 6B, pErk accumulated retrogradely at the ligation site in wild-type but not in *vimentin*^{-/-} sciatic nerve. Erk and Elk1 phosphorylation were subsequently examined in ganglia from wild-type or *vimentin*^{-/-} mice, after lesion of the nerve close to the entry points to the DRG (Figure 6C). In these experiments, phosphorylated Erks appeared in wild-type ganglia from 10 min after the crush, and Elk1 phosphorylation kinetics was similar to that of the Erks. In contrast, ganglia from *vimentin*^{-/-} mice exhibited little or no Erk or Elk1 phosphorylation over the time course of these experiments (Figure 6C). Because Western blots of ganglia were by necessity conducted from whole ganglion lysates, we verified that the observed Elk1 phosphorylation occurs within neurons by immunostaining of ganglion sections. As shown in Figure 6D, Elk1 phosphorylation is concentrated in nuclei of NFH-positive neuronal cell bodies from wild-type animals but is not observed in corresponding neurons from vimentin nulls.

In order to assess the contribution of pErk and vimentin to the cell body response to injury, we proceeded to examine in vitro regenerative outgrowth of adult DRG neurons from *vimentin*^{-/-} mice. Neurite outgrowth from *vimentin*^{-/-} cells 48 hr in culture was significantly reduced compared to wild-type neurons, and
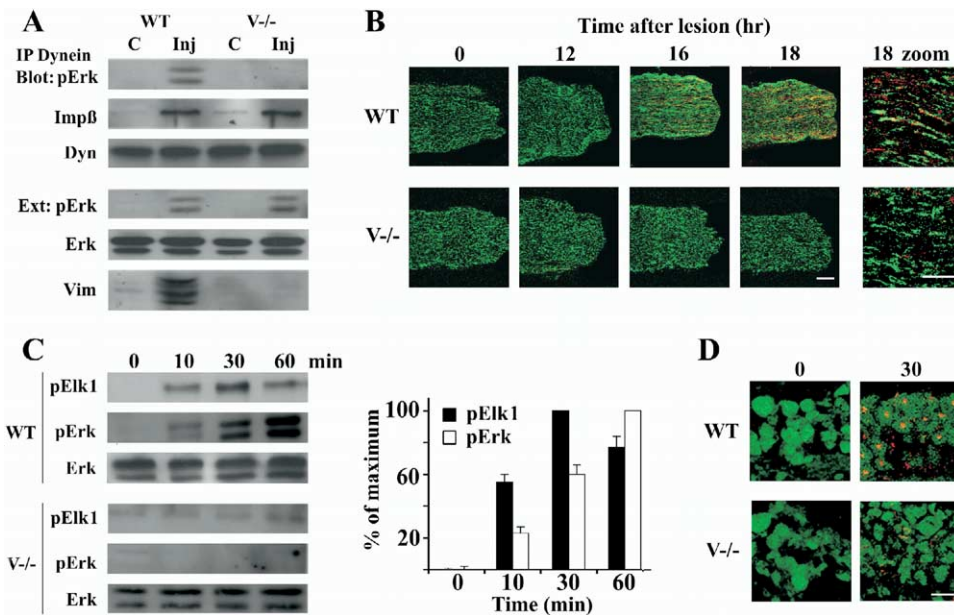
Figure 6. Retrograde Transport of pErk and pElk1 Activation in *vimentin*^{−/−} Mice

(A) pErk does not coprecipitate with dynein in sciatic nerve axoplasm from *vimentin*^{−/−} mice. Aliquots (300 μg) of axoplasm from control and 6 hr postlesion nerve were subjected to dynein immunoprecipitation followed by Western blots for the indicated components. Note that, although Erk phosphorylation is comparable in axoplasm of wild-type and *vimentin*^{−/−} mice, there is no interaction of pErk with the dynein complex in *vimentin*^{−/−} mice. This experiment was repeated three times with similar results.

(B) Retrograde accumulation of pErk at a ligation site in injured sciatic nerve. Sciatic nerves of wild-type and *vimentin*^{−/−} mice underwent crush lesion and ligation between the lesion site and the ganglia. At the indicated times, nerves were removed and sectioned longitudinally over the ligation area before staining for NFH (green) and pErk (red). Sections are shown oriented so that the lesioned side is to the left, and the ligation is on the right. Scale bars are 100 μm for the time series and 10 μm for the higher-magnification zoom panel. Note that pErk accumulates at the ligation site in wild-type nerve but not in the vimentin nulls. This experiment was repeated twice with equivalent results.

(C) pErk and pElk1 activation in mouse DRG. DRG processes were lesioned approximately 1 mm from the ganglia. After incubation for the indicated times, ganglia were lysed and subjected to Western blot analyses as shown. Concomitant activation of pErk and pElk1 was observed in ganglia from wild-type but not from *vimentin*^{−/−} mice. The quantification is percent of maximum, average ± standard deviation of three experiments.

(D) Cross-sections of ganglia from the experiment described in (C) immunostained for NFH (green) and pElk1 (red) show pElk1 activation in wild-type but not vimentin null neurons. Scale bar, 50 μm.

the difference was even more pronounced when comparing only the β-gal-positive neurons from the knockout to vimentin-positive neurons from wild-type mice (Figures 7A and 7B). There was no observable difference in outgrowth capacity of vimentin null/β-gal-negative neurons as compared to wild-type/vimentin-negative neurons. Trituration of *vimentin* null neurons with calpain-treated recombinant vimentin rescued the outgrowth deficit in β-gal-positive cells and had no effect on neurons that did not express β-gal, as shown by comparing outgrowth of β-gal-expressing neurons (those originally destined to express vimentin) with similar cells from the same ganglia that did not express β-gal (Figures 7A, 7B, and S2A). We examined the capacity of calpain-treated vimentin for polymerization by comparing pelleted versus soluble vimentin after ultracentrifugation (Figure S2B) and by comparative observation of vimentin filaments by electron microscopy (Figure S2C). Both assays showed that calpain-treated vimentin was not capable of polymerizing into filamentous structures; thus, the outgrowth rescue activity obtained by trituration of the protein cannot be due to cytoskeletal roles of vimentin.

DRG neurons undergo a transcription-dependent switch from arborizing to long-distance neurite outgrowth upon peripheral axotomy by a previous (conditioning) lesion of the sciatic nerve (Smith and Skene, 1997), and this effect is mediated by the retrograde signaling complex (Hanz et al., 2003). We therefore examined the conditioning lesion response in DRG of *vimentin*^{−/−} mice. Sciatic nerve crush was performed 3 days prior to culture of neurons from the L4/L5 DRGs of vimentin null and wild-type mice. After 18 hr in culture, prelesioned conditioned neurons from wild-type mice extended neurites that were on average 2-fold longer than those of naive controls (Figures 7C and 7D). A similar effect was observed in neurons from *vimentin* null mice that did not express β-gal. In contrast, β-gal-positive neurons from *vimentin*^{−/−} DRG did not extend longer neurites as a result of the conditioning crush (Figures 7C and 7D). Thus, both in vitro and in vivo, a vimentin-mediated signal facilitates the regenerative response of DRG neurons.

In order to ask whether the vimentin-mediated signal is pErk, we tested a series of synthetic peptides designed to mimic surface-exposed regions of Erk for their capacity to interfere with pErk-vimentin binding (Figure 7E). Out of five peptides examined in this way, a
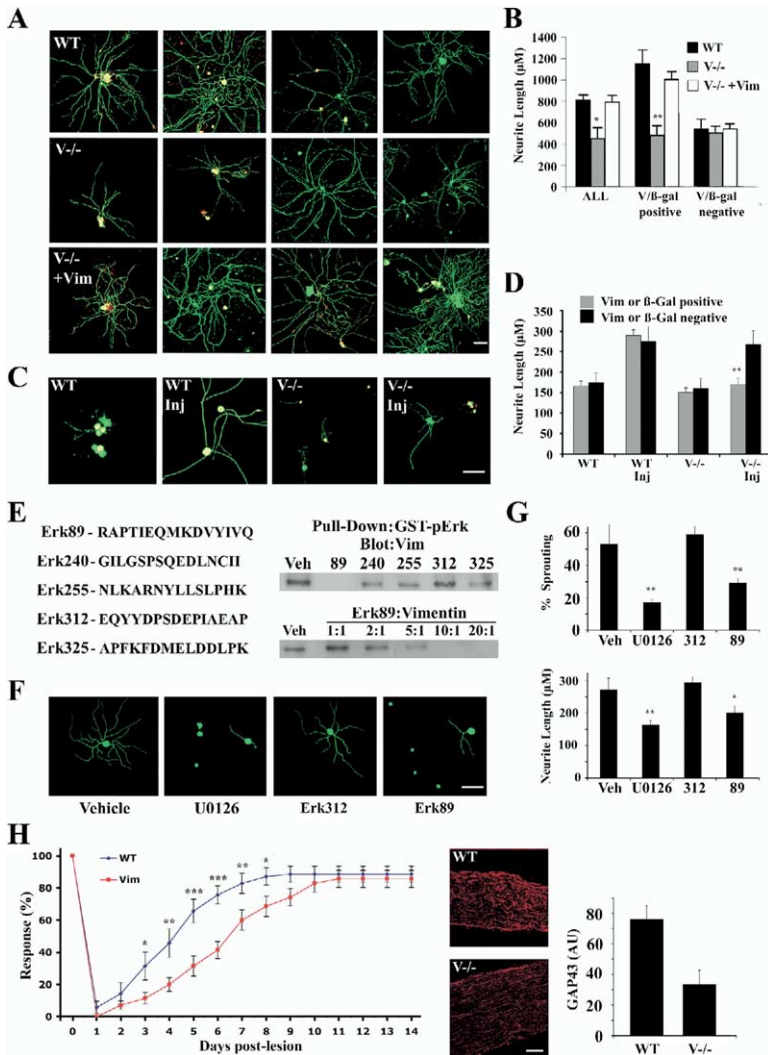
Figure 7. Neurite Outgrowth and Regeneration Responses to Vimentin and pErk

(A and B) Comparison of outgrowth of adult mice DRG neurons after 48 hr in culture. Green indicates immunostaining for NFH, and red indicates vimentin (wild-type) or β-gal (vimentin⁻/⁻). Each row includes two panels with predominantly vimentin- or β-gal-positive cells and two panels with cells predominantly negative for these markers. The third (lower) row shows vimentin⁻/⁻ neurons triturated with calpain-cleaved vimentin (6.7 μg per ganglion) before plating. Quantification of three independent experiments is shown in (B), measuring at least 250 cells per experiment (average ± standard error of mean). Significant differences are revealed in neurite outgrowth between the vimentin null and wild-type neurons in the total population (p < 0.05). These differences are even more pronounced when comparing vimentin-positive to β-gal-positive neurons (p < 0.01), while there was no difference between wild-type vimentin-negative and vimentin null β-gal-negative cells. Trituration of calpain-treated vimentin to vimentin null neurons before plating enhanced the outgrowth of β-gal-positive cells and had no effect on cells that did not express the β-gal marker. Vimentin uptake after trituration was verified by immunostaining, and we analyzed only those cultures in which over 50% of the cells contained vimentin 3 hr after trituration. Trituration of calpain-treated neurofilament had no effect, and calpain-treated vimentin was found to be incapable of polymerization (Figure S2). Scale bar, 50 μm.

(C and D) Effects of sciatic nerve conditional lesion in vimentin⁻/⁻ mice. Sciatic nerves were crushed as described, and L4/L5 DRG neurons were cultured 3 days after the conditioning lesion. Neurons were fixed after 18 hr in culture and stained, and neurite outgrowth was measured. Wild-type neurons and vimentin null neurons negative for β-gal revealed accelerated neurite outgrowth after a conditioning crush (>100 neurons measured from two independent experiments; p < 0.01), whereas no change was observed in vimentin null β-gal-positive cells (250 neurons measured from two independent experiments; average ± standard error of mean). Scale bar, 100 μm.

(E) Effects of five Erk-derived synthetic peptides (sequences shown on the left) on the interaction of vimentin with pErk. Five different peptides were incubated with vimentin (20:1 molar ratio) in PBS for 2 hr at 37°C, followed by GST-pErk pull-down. A single peptide designated Erk89 clearly inhibits pErk-vimentin binding, and the inhibition was shown to be concentration dependent. This experiment was repeated three times with similar results.

(F and G) Effects of the MEK inhibitor UO126 and the Erk89 peptide on conditioning lesion responses in adult rat DRG neurons. Sciatic nerves were injected with 10 μM UO126 or 250 μg of Erk89 or Erk312 peptides, concomitantly with a conditioning crush injury. Five days after the lesion, L4/L5 DRG neurons were cultured in vitro for 18 hr, fixed, and stained for NFH before measurement of neurite outgrowth. Both the percentage of sprouting neurons (n = 300 for each treatment; p < 0.01) and the neurite length in those that did sprout (n > 60 for each treatment; p < 0.05) were significantly reduced by UO126 or Erk89, whereas the Erk312 peptide had no effect. The experiment was repeated three times with two animals for each treatment, totaling six independent animal assays for each treatment (average ± standard error of mean). Scale bar, 100 μm.

(H) Recovery of sensory responses after lesion of the sciatic nerve in vivo. Wild-type and vimentin null mice (14 animals in each group) underwent sciatic nerve lesion and were then monitored daily for up to 30 days postlesion. At each monitoring session, the animal's response to toe pinch was tested for each individual digit, and the response was plotted as percent of responding digits. There was an immediate and essentially complete cessation of response in both groups of animals immediately after the lesion, with a clear difference in recovery kinetics between wild-type and vimentin null animals. GAP43 immunostaining was performed to compare (AU, arbitrary units) regeneration in longitudinal sections totaling 1 cm nerve length adjacent to the lesion site. This analysis revealed significant differences between wild-type and vimentin null nerves 6 days after lesion (average ± standard deviation). Scale bar, 100 μm.

single peptide designated Erk89 (numbering is the first residue of the peptide as found in human Erk2) was found to inhibit vimentin-pErk binding in a concentration-dependent manner. We therefore tested the effects of the Erk89 in comparison with another one of the peptides on the conditioning lesion response in adult rats. In parallel experiments, we also examined the effects of the MEK inhibitor UO126. The peptides or the inhibitor were injected into sciatic nerve concomitantly with a conditioning sciatic nerve crush, and outgrowth of
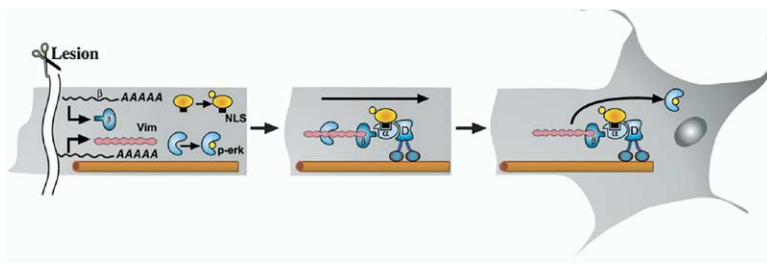
Figure 8. A Model for Vimentin-Dependent Retrograde Transport of Phosphorylated MAP Kinases

Local synthesis of vimentin at the axonal lesion site (left), together with phosphorylation of Erk (yellow), allows linkage of pErk to the retrograde complex via a direct interaction of vimentin with importin β. The complex may protect pErk from phosphatases due to steric hindrance, and pErk should remain bound to vimentin as long as the complex is within a high-calcium microenvironment. Upon arrival in the cell body, pErk dissociates from vimentin and is then available to downstream targets in the cell body or the nucleus.

L4/L5 DRG neurons was examined 5 days later. Both UO126 and Erk89 significantly inhibited the conditioning lesion response in rat DRG neurons, whereas the Erk312 peptide had no effect (Figures 7F and 7G). The UO126 results show that pErk is required for efficient retrograde injury signaling, and the effects of the Erk89 peptide indicate that vimentin-pErk binding is necessary for the process. Taken together with the results obtained from vimentin null mice, this series of experiments proves that vimentin-mediated retrograde transport of pErk facilitates the cell body response in the sciatic nerve-DRG system.

Finally, we examined the effects of vimentin on sensory neuron regeneration in vivo. Sciatic nerve crush was carried out on 14 wild-type and 14 *vimentin*$^{-/-}$ mice, followed by daily monitoring of responses to toe pinch for up to 30 days postlesion. As shown in Figure 7H, there was an immediate and essentially complete cessation of sensory response in both groups immediately after the lesion. Recovery of sensation was delayed in the *vimentin* null animals as compared to wild-type, with full recovery observed after 11 days in null animals compared to 1 week in wild-type. Quantification of regenerative sprouting by GAP43 immunostaining of longitudinal sections revealed significant differences between wild-type and *vimentin* null nerves 3–9 days after lesion (Figure 7H and data not shown). Thus, lack of vimentin causes a marked delay in the in vivo regeneration of sensory axons in sciatic nerve.

Discussion

We have shown that vimentin is upregulated in sciatic nerve axoplasm after lesion and is transported in the retrograde injury-signaling complex via a direct interaction with importin β. The MAP kinases Erk1 and Erk2 are phosphorylated in axoplasm after nerve lesion, and vimentin binds phosphorylated Erks, thus linking them to the retrograde transport system (Figure 8). These findings reveal how non-NLS-bearing signaling molecules can access the importins-mediated retrograde transport complex, describe an additional role for intermediate filaments, and define a mechanism that allows long-distance kinase signaling within cells.

Recruitment of Vimentin to the Retrograde Transport Machinery

A critical initiating event for the mechanism outlined above is local axonal synthesis of both importin β and vimentin at the lesion site. Recently, it has become apparent that local axonal translation occurs for a wide range of gene products, contributing to diverse processes of growth cone navigation in the embryonic nervous system or regeneration in the adult (Giuditta et al., 2002). Thus, local translation of specific axonal transcripts provides a versatile mechanism activating latent signaling mechanisms. Indeed, local translation might be a prerequisite for vimentin participation in retrograde injury signaling, as anterograde transport of the protein from the cell body may be diverted to filament assembly en route (Prahlad et al., 1998). *vimentin* mRNA is known to be targeted to specific subcellular locations in nonneuronal cells (Morris et al., 2000), and it will be interesting to determine how vimentin message is targeted to axons. In this context, it is noteworthy that vimentin synthesis at an axonal lesion site introduces the nascent protein chain directly into an elevated calcium environment likely to be unfavorable for filament assembly. High calcium may inhibit filament assembly due to vimentin phosphorylation by calcium-activated CAM kinase II (Inagaki et al., 1997), or due to calpain-mediated cleavage of vimentin.

Potential Regulatory Roles for Calcium

The in vitro effects of calcium on pErk binding, and phosphatase protection, suggest that calcium elevation in the nerve is likely to influence the retrograde signal. Calcium is elevated in axons of both invertebrates and vertebrates after nerve injury or trauma (Mandolesi et al., 2004; Ziv and Spira, 1995). Although recovery of axonal calcium to basal levels can be fairly rapid in invertebrate neurons in culture (Ziv and Spira, 1995), levels in injured mammalian nerve may remain elevated for prolonged periods (Iwata et al., 2004; Wolf et al., 2001). This might be due to delayed sealing caused by reduced extracellular calcium in the mammalian system (Shi et al., 2000; Yoo et al., 2003), or due to different rates of sealing in axons of different diameters (Howard et al., 1999). Thus, an axonal lesion may lead to significant and prolonged elevation of calcium levels in the axon, thereby facilitating the interaction of pErk with vimentin. If the injury is severe, axonal sealing may be delayed, and calcium elevation might be maintained for sufficient time for the pErk signal to arrive at the cell body. If the injury is relatively mild and axon sealing and calcium recovery is rapid, pErk may dissociate before arrival at the cell body.

Mobility of Vimentin—Additional Roles
for Intermediate Filaments

Our data reveal unexpected roles for *vimentin* that are not necessarily related to its functions in cytoskeleton formation. Initial studies on *vimentin* null mice showed that they survive and breed normally (Colucci-Guyon et al., 1994). Subsequent analyses revealed subtle defects in cerebellar glia (Gimenez y Ribotta et al., 2000), neurobehavioral effects (Lalonde and Strazielle, 2003), and impaired skin wound healing due to mesenchymal defects (Eckes et al., 2000); thus, *vimentin* is important in a range of cell types. A recent study has shown reduced astroglial reactivity and increased plastic sprouting of supraspinal axons in hemisected spinal cord of *vimentin/GFAP* double null mice (Menet et al., 2003). This phenotype was attributed to a reduction of the inhospitable environment that would normally be generated by astrocytes at the lesion site. The outcome of *vimentin* perturbation in nerve injury is therefore likely to depend on the balance between its regeneration-enhancing contribution to intrinsic growth mechanisms via retrograde axonal signaling versus an indirect regeneration-inhibiting influence, due to its major structural role in astroglial cells.

Our data also shed light on mechanisms of vimentin movement within cells. Live imaging of cells expressing GFP-vimentin has shown that vimentin is found in complexes of various sizes, which move bidirectionally on microtubules (Ho et al., 1998; Prahlad et al., 1998; Yoon et al., 1998). Conventional kinesin is thought to move vimentin outward toward plus ends of microtubules (Prahlad et al., 1998), and dynamitin overexpression was recently used to demonstrate a role for dynein in inward minus end-directed movement of vimentin on microtubules (Clarke and Allan, 2002; Helfand et al., 2002). The direct interaction between vimentin and importin β allows vimentin to connect to dynein via the association of importins with dynein (Hanz et al., 2003). Moreover, these findings may rationalize some previously puzzling reports showing vimentin concentration in the cell center upon disruption of microtubules (Clarke and Allan, 2002; Gurland and Gundersen, 1995; Yoon et al., 1998). Inward clustering of vimentin at the cell center may be due to interactions of importin β with nucleoporins. An importin β-nucleoporin interaction also provides a mechanism for vimentin entry to the nucleus, strengthening the argument for possible nuclear roles of vimentin (Traub and Shoeman, 1994). These findings expand the range of potential roles for *vimentin* and suggest that intermediate filaments provide dynamic and mobile scaffolds for localization and long-distance transport of signaling molecules within cells.

pErk and Other Signals
in the Regenerative Response

Our data show that vimentin modulates regeneration in a subset of DRG neurons; however, *vimentin* is not expressed in approximately 40% of the neuronal population. Since retrograde transport of pErk in injured sciatic nerve is completely dependent on vimentin, other signals most likely substitute or compensate for pErk in *vimentin*-negative cells. We have previously shown that retrograde injury signaling can be inhibited by excess NLS peptides (Hanz et al., 2003), and since NLS peptides did not interfere with the vimentin-pErk interaction, additional signaling molecules are likely transported by the importin α classical NLS binding site in the complex. Conversely, a different kinase signal may be transported instead of pErk in *vimentin* null cells; for example, there is evidence for activation of the jnk pathway in injured rat DRG axons (Kenney and Kocsis, 1998) and of protein kinase G in lesioned *Aplysia* neurons (Sung et al., 2004). Interestingly, trk receptor activation by NGF leads to retrograde signaling via Erk5, and not Erk1/2 (Watson et al., 2001). Thus it is becoming apparent that retrograde signaling occurs via a diversity of signals, depending on the neuronal subtype and type of stimulus.

Although vimentin is known to bind other signaling molecules, such as PLA2 (Paramio and Jorcano, 2002), we have focused on the role of vimentin-transported pErk in lesioned sciatic nerve. How might pErk contribute to enhanced regeneration of sensory neurons? Two independent studies have shown that elevation of cAMP levels in the DRG mimics the regeneration-inducing effect of a conditioning lesion (Neumann et al., 2002; Qiu et al., 2002). Cross-talk between the cAMP and Erk pathways can occur via inhibition of cAMP phospho-diesterase-4 isoforms by Erk, thus increasing cAMP levels in the cell (Houslay and Baillie, 2003). Indeed, it has recently been shown that Erk activated by neurotrophin receptors transiently inhibits cAMP phospho-diesterase-4 in DRG neurons (Gao et al., 2003). The transient nature of the inhibition may be due to activation of cAMP-dependent PKA, which in turn can lead to inhibition of the Erk pathway (Houslay and Baillie, 2003; Maeda et al., 2004). Thus, ongoing elevation of cAMP in the cell body may require a supply of newly phosphorylated Erk, provided by vimentin-mediated trafficking from the axon. It will be interesting to determine how direct effects of pErk on transcription factors like Elk1 are combined with indirect effects via cAMP or other second messengers to coordinate neuronal regeneration. In this context, it is noteworthy that Liu and Snider (2001) showed that application of a MEK inhibitor to adult DRG neurons in culture had no effect on their regenerative outgrowth. In that case, the neurons underwent conditional lesioning in vivo and were exposed to the MEK inhibitor only afterward in the culture. Taken together with our findings, this indicates that pErk is involved in the retrograde signal initiating regeneration but is not required during subsequent outgrowth.

Long-Distance Transport of Kinase Signals

This paper has addressed the issue of how kinase signals might be propagated over long distances within a cell. Most previous work in this field was on signals initiated at the plasma membrane by receptor tyrosine kinases, thus naturally leading to a focus on mechanisms allowing lateral propagation in the membrane or intracellular trafficking of membrane-enclosed vesicles. Although soluble complexes of dynein-trafficked molecules have been recognized especially in neurons (Guzik and Goldstein, 2004; Hanz and Fainzilber, 2004; Hirokawa and Takemura, 2004), it was not clear how such

complexes could maintain integrity of an activated kinase while traversing a phosphatase-rich environment. We suggest a mechanism that enables the cell to transport an activated kinase over distances of many centimeters in a lesioned axon. A combination of local translation and calpain cleavage produces a soluble intermediate filament fragment that may bind the activated kinase under high-calcium conditions and release it with signaling moiety intact upon arrival at a low-calcium region. Linkage of the intermediate filament-kinase complex to the retrograde transport machinery is via a cotranslated importin, thus providing additional specificity to the system. The versatility of this mechanism suggests that vimentin and pErk may turn out to be one of many kinase translocation partnerships.

Experimental Procedures

Animals, In Vivo Procedures, and Cultures
Adult (8–12 weeks old) male Wistar rats were purchased from Harlan, Inc. (Rehovot, Israel). Wild-type or *vimentin*$^{-/-}$ SV129 mice with β-gal inserted at the vimentin locus were generously provided by Dr. E Colucci-Guyon (Pasteur Institute) and bred and maintained at the Veterinary Resources Department of the Weizmann Institute as previously described (Colucci-Guyon et al., 1994). Sciatic nerve crush was performed as previously described (Hanz et al., 2003). Axoplasm was obtained from freshly dissected nerves after gentle compression in phosphate-buffered saline (PBS) or in nuclear transport buffer (NTB; Hanz et al., 2003) without EGTA, containing protease inhibitors (Roche) and 1 mM orthovanadate when necessary. Purity of axoplasm was verified by Western blotting for Schwann cell (S-100) and nuclear (RCC1) markers as described by Hanz et al. (2003) and other glial markers as indicated in Figure S1. DRG cultures from adult animals were as previously described (Hanz et al., 2003). Vimentin trituration into DRGs was carried out by introducing 100 μg of vimentin to the trituration medium for 15 ganglia. Vimentin was prepared for trituration by cleavage with calpain (100 μU; 2 hr). In vivo conditioning sciatic nerve lesions were carried out as described by Hanz et al. (2003). For tests of introduced substances, sciatic nerves were injected concomitantly with the crush with the MEK inhibitor UO126 (Biomol; 10 μM), the Erk89 or Erk312 peptides (250 μg), or calpeptin (Calbiochem; 100 μM). L4/L5 DRG neurons were cultured 3–5 days after the conditioning lesion. Neurons were fixed after 18 hr in culture and stained with NFH, and the length of the longest axon per neuron was measured. In vivo regeneration and recovery of sensory function was tested on wild-type and vimentin null mice following sciatic nerve crush. Mice were monitored daily for foot withdrawal in response to toe pinch of each individual digit with forceps, scored as the percentage of responding digits. Longitudinal sections on injured nerve were carried out at designated times and immunostained with anti-GAP43 rabbit polyclonal AB5220 (Chemicon). All animal experimentation was under the supervision of the Weizmann Institute Institutional Animal Care and Use Committee.

Antibodies, Western Blots, and Immunofluorescence
The following antibodies were from Chemicon International (Temecula, CA): vimentin monoclonal clone V9 MAB3400; vimentin polyclonal AB1620; peripherin polyclonal AB1530; dynein 74 kDa intermediate chain monoclonal MAB1618; β-gal monoclonal AB1802; β-gal polyclonal AB1211; NFH polyclonal AB1989; CNPase monoclonal MAB326. The following antibodies were from Sigma (Rehovot, Israel): NFH clone N52 monoclonal; Erk polyclonal M5670; doubly phosphorylated Erk monoclonal M8159; GFAP clone G-A-5. The importin β monoclonal antibody 3E9 MA3-070 was from Affinity Bioreagents (Golden, CO); β-tubulin polyclonal SC 9104 and lamin A/C N18 SC 6215 were from Santa Cruz (Santa Cruz, CA); for pElk-1 we used monoclonal 9186 from Cell Signaling (Beverley, MA); and anti-importin α4 was a kind gift from Dr. Karsten Weis (UC Berkeley). HRP-conjugated secondary antibodies were from

BioRad, and fluorescent secondary antibodies were from Jackson ImmunoResearch. Western blots and immunostainings were carried out as described in Hanz et al. (2003). For Westerns, axoplasm samples were resolved on 10% SDS-PAGE, transferred to nitrocellulose, and after reaction with the desired antibodies were developed with ECL (Pierce). For immunofluorescence, DRG neurons were fixed with 3% paraformaldehyde, while control and injured sciatic nerve segments were fixed in 4% paraformaldehyde, frozen with Tissue-Tek (Sakura, Tokyo), and sectioned longitudinally at 10 μm thickness in a Leica cryostat. Neuron cultures and sciatic nerve sections were mounted in moviol (Calbiochem) and observed under an Olympus FV500 confocal laser scanning microscope. For Rhodamine RED-X and Cy5 visualization, we used 543 nm and 633 nm wavelengths in a sequential manner.

Recombinant Expression of pERK and Importin β
To obtain doubly phosphorylated ERK, activated human GST-ERK2 was coexpressed with constitutively active MEK1 in BL21 bacteria, as previously described (Wilsbacher and Cobb, 2001). The bacteria were grown in 2YT medium at 30°C to an optical density of 0.6, and then 1 mM IPTG was added for an additional 4 hr. GST-importin β and His-tagged importin β constructs were kindly provided by Dr. Steve Adam (Northwestern University, Chicago, IL) and Dr. Ziv Reich (Weizmann Institute), respectively. Importin β constructs were grown in BL21 bacteria in Luria-Bertani medium at 37°C until OD 0.5, followed by overnight incubation with 100 μM IPTG at 26°C. Proteins were purified over Glutathione-Sepharose 4B (Amersham Biosciences) or nickel-NTA agarose (Qiagene) according to the manufacturer's instructions.

Pull-Downs and Coimmunoprecipitations
Sciatic nerve axoplasm (500 μg) was precleared for 1 hr with 80% protein G-Sepharose (Amersham Bioscience). Following overnight incubation with primary antibody, complexes were incubated on protein G beads for 2 hr, washed extensively, and eluted by boiling in SDS-PAGE sample buffer before loading on gels for Western blot analyses. For coimmunoprecipitation in the presence of competitors, 2 μM NLS or reverse-NLS peptides were added to the axoplasm for overnight incubation at 4°C. For direct pull-downs, GST-pERK (0.5 μg) or importin β (1 μg) were equilibrated in PBS or NTB and added to 500 μg aliquots of axoplasm from different postlesion times. Direct interactions were tested in vitro by mixing 0.1 μg recombinant Syrian hamster vimentin or NF (Cytoskeleton Inc., Denver, CO) to GST-pERK or GST-importin β and incubated for 2 hr at 37°C. All pull-downs were washed twice with 0.2 M NaCl in PBS or NTB and twice again with PBS or NTB before elution in SDS-PAGE sample buffer for loading on gels.

Phosphatase Protection Assay
His-Imp-β (2 μg) was incubated with GST-pERK (0.1 μg) and with 0–2 μg vimentin or NF for 2 hr at 37°C. AP (2 units; Roche, Mannheim, Germany) or axoplasm from injured nerve (100 μg) was then added for an additional 30 min. Complexes were purified over GST beads followed by Western blot analysis for pERK. AP activity was verified with the synthetic substrate pNPP (Sigma S0942) dissolved in 0.1 M glycine buffer (0.1 M glycine, 1 mM MgCl$_2$, 1 mM ZnCl$_2$; pH 10.4) for a stock solution of 1 mg/ml. One unit AP was added to a reaction mixture consisting of 1 μg pNPP with 2 μg vimentin or NF in Tris buffer (pH 7.5) and incubated for 5, 15, and 30 min before stopping the reaction with 3 N NaOH. The yellow hydrolysis product was quantified spectrophotometrically at 405 nm.

Retrograde Movement
Rat sciatic nerves were crushed and dissected out at increasing times after lesion (0–24 hr). Dissected nerves were divided into consecutive segments of about 10 mm each before extraction of axoplasm. From each segment, 300 μg axoplasm was immunoprecipitated with the dynein antibody, and precipitates were analyzed by Western blot for vimentin and pErk. Followup experiments in mouse were conducted with wild-type or *vimentin*$^{-/-}$ sciatic nerves, crushed and ligated as described. At designated times, the nerves were dissected, fixed, and sectioned longitudinally over the ligation

as previously described (Hanz et al., 2003). Sections were then immunostained for pErk and NFH.

pElk1 Response

Rat L4/L5 DRGs were dissected 0–24 hr after sciatic nerve lesion into lysis buffer (50 mM Tris-HCL [pH 7.4], 150 mM NaCl, 1 mM PMSF, 1 mM EDTA, 1% Triton X-100, and protease inhibitor cocktail [Roche]) and processed for Western blot of pErk and pElk-1. For pElk1 analysis in mouse, DRG processes were lesioned at about 1 mm distance from the ganglia before transfer to PBS and incubation in vitro for up to 1 hr at 37°C, followed by lysis and Western blot analysis.

Supplemental Data

The Supplemental Data include two figures and can be found with this article online at http://www.neuron.org/cgi/content/full/45/5/715/DC1/.

References

Boyne, L.J., Fischer, I., and Shea, T.B. (1996). Role of vimentin in early stages of neuritogenesis in cultured hippocampal neurons. Int. J. Dev. Neurosci. *14*, 739–748.

Clarke, E.J., and Allan, V. (2002). Intermediate filaments: vimentin moves in. Curr. Biol. *12,* R596–R598.

Colucci-Guyon, E., Portier, M.M., Dunia, I., Paulin, D., Pournin, S., and Babinet, C. (1994). Mice lacking vimentin develop and reproduce without an obvious phenotype. Cell *79*, 679–694.

Dubey, M., Hoda, S., Chan, W.K., Pimenta, A., Ortiz, D.D., and Shea, T.B. (2004). Reexpression of vimentin in differentiated neuroblastoma cells enhances elongation of axonal neurites. J. Neurosci. Res. *78*, 245–249.

Eckes, B., Colucci-Guyon, E., Smola, H., Nodder, S., Babinet, C., Krieg, T., and Martin, P. (2000). Impaired wound healing in embryonic and adult mice lacking vimentin. J. Cell Sci. *113*, 2455–2462.

Gao, Y., Nikulina, E., Mellado, W., and Filbin, M.T. (2003). Neurotrophins elevate cAMP to reach a threshold required to overcome inhibition by MAG through extracellular signal-regulated kinase-dependent inhibition of phosphodiesterase. J. Neurosci. *23*, 11770–11777.

Gimenez y Ribotta, M., Langa, F., Menet, V., and Privat, A. (2000). Comparative anatomy of the cerebellar cortex in mice lacking vimentin, GFAP, and both vimentin and GFAP. Glia *31*, 69–83.

Giuditta, A., Kaplan, B.B., van Minnen, J., Alvarez, J., and Koenig, E. (2002). Axonal and presynaptic protein synthesis: new insights into the biology of the neuron. Trends Neurosci. *25*, 400–404.

Goldberg, J.L. (2003). How does an axon grow? Genes Dev. *17*, 941–958.

Gurland, G., and Gundersen, G.G. (1995). Stable, detyrosinated microtubules function to localize vimentin intermediate filaments in fibroblasts. J. Cell Biol. *131*, 1275–1290.

Guzik, B.W., and Goldstein, L.S. (2004). Microtubule-dependent transport in neurons: steps towards an understanding of regulation, function and dysfunction. Curr. Opin. Cell Biol. *16*, 443–450.

Hanz, S., and Fainzilber, M. (2004). Integration of retrograde axonal and nuclear transport mechanisms in neurons: implications for therapeutics. Neuroscientist *10*, 404–408.

Hanz, S., Perlson, E., Willis, D., Zheng, J.Q., Massarwa, R., Huerta, J.J., Koltzenburg, M., Kohler, M., van-Minnen, J., Twiss, J.L., and Fainzilber, M. (2003). Axoplasmic importins enable retrograde injury signaling in lesioned nerve. Neuron *40*, 1095–1104.

Harel, A., and Forbes, D.J. (2004). Importin beta: conducting a much larger cellular symphony. Mol. Cell *16*, 319–330.

Helfand, B.T., Mikami, A., Vallee, R.B., and Goldman, R.D. (2002). A requirement for cytoplasmic dynein and dynactin in intermediate filament network assembly and organization. J. Cell Biol. *157*, 795–806.

Hirokawa, N., and Takemura, R. (2004). Molecular motors in neuronal development, intracellular transport and diseases. Curr. Opin. Neurobiol. *14*, 564–573.

Ho, C.L., Martys, J.L., Mikhailov, A., Gundersen, G.G., and Liem, R.K. (1998). Novel features of intermediate filament dynamics revealed by green fluorescent protein chimeras. J. Cell Sci. *111*, 1767–1778.

Houslay, M.D., and Baillie, G.S. (2003). The role of ERK2 docking and phosphorylation of PDE4 cAMP phosphodiesterase isoforms in mediating cross-talk between the cAMP and ERK signalling pathways. Biochem. Soc. Trans. *31*, 1186–1190.

Howard, M.J., David, G., and Barrett, J.N. (1999). Resealing of transected myelinated mammalian axons in vivo: evidence for involvement of calpain. Neuroscience *93*, 807–815.

Howe, C.L., and Mobley, W.C. (2004). Signaling endosome hypothesis: A cellular mechanism for long distance communication. J. Neurobiol. *58*, 207–216.

Inagaki, N., Goto, H., Ogawara, M., Nishi, Y., Ando, S., and Inagaki, M. (1997). Spatial patterns of Ca2+ signals define intracellular distribution of a signaling by Ca2+/Calmodulin-dependent protein kinase II. J. Biol. Chem. *272*, 25195–25199.

Iwata, A., Stys, P.K., Wolf, J.A., Chen, X.H., Taylor, A.G., Meaney, D.F., and Smith, D.H. (2004). Traumatic axonal injury induces proteolytic cleavage of the voltage-gated sodium channels modulated by tetrodotoxin and protease inhibitors. J. Neurosci. *24*, 4605–4613.

Kenney, A.M., and Kocsis, J.D. (1998). Peripheral axotomy induces long-term c-Jun amino-terminal kinase-1 activation and activator protein-1 binding activity by c-Jun and junD in adult rat dorsal root ganglia in vivo. J. Neurosci. *18*, 1318–1328.

Kholodenko, B.N. (2003). Four-dimensional organization of protein kinase signaling cascades: the roles of diffusion, endocytosis and molecular motors. J. Exp. Biol. *206*, 2073–2082.

Lalonde, R., and Strazielle, C. (2003). Neurobehavioral characteristics of mice with modified intermediate filament genes. Rev. Neurosci. *14*, 369–385.

Lariviere, R.C., and Julien, J.P. (2004). Functions of intermediate filaments in neuronal development and disease. J. Neurobiol. *58*, 131–148.

Liu, R.Y., and Snider, W.D. (2001). Different signaling pathways mediate regenerative versus developmental sensory axon growth. J. Neurosci. *21*, RC164.

Maeda, M., Lu, S., Shaulsky, G., Miyazaki, Y., Kuwayama, H., Tanaka, Y., Kuspa, A., and Loomis, W.F. (2004). Periodic signaling controlled by an oscillatory circuit that includes protein kinases ERK2 and PKA. Science *304*, 875–878.

Mandolesi, G., Madeddu, F., Bozzi, Y., Maffei, L., and Ratto, G.M. (2004). Acute physiological response of mammalian central neurons to axotomy: ionic regulation and electrical activity. FASEB J. *18*, 1934–1936.

Menet, V., Prieto, M., Privat, A., and Gimenez y Ribotta, M. (2003).

Axonal plasticity and functional recovery after spinal cord injury in mice deficient in both glial fibrillary acidic protein and vimentin genes. Proc. Natl. Acad. Sci. USA *100*, 8999–9004.

Morris, E.J., Evason, K., Wiand, C., L'Ecuyer, T.J., and Fulton, A.B. (2000). Misdirected vimentin messenger RNA alters cell morphology and motility. J. Cell Sci. *113*, 2433–2443.

Neumann, S., Bradke, F., Tessier-Lavigne, M., and Basbaum, A.I. (2002). Regeneration of sensory axons within the injured spinal cord induced by intraganglionic cAMP elevation. Neuron *34*, 885–893.

Paramio, J.M., and Jorcano, J.L. (2002). Beyond structure: do intermediate filaments modulate cell signalling? Bioessays *24*, 836–844.

Perlson, E., Hanz, S., Medzihradszky, K.F., Burlingame, A.L., and Fainzilber, M. (2004a). From snails to sciatic nerve: Retrograde injury signaling from axon to soma in lesioned neurons. J. Neurobiol. *58*, 287–294.

Perlson, E., Medzihradszky, K.F., Darula, Z., Munno, D.W., Syed, N.I., Burlingame, A.L., and Fainzilber, M. (2004b). Differential proteomics reveals multiple components in retrogradely transported axoplasm after nerve injury. Mol. Cell. Proteomics *3*, 510–520.

Prahlad, V., Yoon, M., Moir, R.D., Vale, R.D., and Goldman, R.D. (1998). Rapid movements of vimentin on microtubule tracks: kinesin-dependent assembly of intermediate filament networks. J. Cell Biol. *143*, 159–170.

Qiu, J., Cai, D., Dai, H., McAtee, M., Hoffman, P.N., Bregman, B.S., and Filbin, M.T. (2002). Spinal axon regeneration induced by elevation of cyclic AMP. Neuron *34*, 895–903.

Reynolds, A.R., Tischer, C., Verveer, P.J., Rocks, O., and Bastiaens, P.I. (2003). EGFR activation coupled to inhibition of tyrosine phosphatases causes lateral signal propagation. Nat. Cell Biol. *5*, 447–453.

Rogers, K.R., Eckelt, A., Nimmrich, V., Janssen, K.P., Schliwa, M., Herrmann, H., and Franke, W.W. (1995). Truncation mutagenesis of the non-alpha-helical carboxyterminal tail domain of vimentin reveals contributions to cellular localization but not to filament assembly. Eur. J. Cell Biol. *66*, 136–150.

Shi, R., Asano, T., Vining, N.C., and Blight, A.R. (2000). Control of membrane sealing in injured mammalian spinal cord axons. J. Neurophysiol. *84*, 1763–1769.

Smith, D.S., and Skene, J.H. (1997). A transcription-dependent switch controls competence of adult neurons for distinct modes of axon growth. J. Neurosci. *17*, 646–658.

Sung, Y.J., Povelones, M., and Ambron, R.T. (2001). RISK-1: a novel MAPK homologue in axoplasm that is activated and retrogradely transported after nerve injury. J. Neurobiol. *47*, 67–79.

Sung, Y.J., Walters, E.T., and Ambron, R.T. (2004). A neuronal isoform of protein kinase G couples mitogen-activated protein kinase nuclear import to axotomy-induced long-term hyperexcitability in Aplysia sensory neurons. J. Neurosci. *24*, 7583–7595.

Traub, P., and Shoeman, R.L. (1994). Intermediate filament proteins: cytoskeletal elements with gene-regulatory function? Int. Rev. Cytol. *154*, 1–103.

Watson, F.L., Heerssen, H.M., Bhattacharyya, A., Klesse, L., Lin, M.Z., and Segal, R.A. (2001). Neurotrophins use the Erk5 pathway to mediate a retrograde survival response. Nat. Neurosci. *4*, 981–988.

Weible, M.W., and Hendry, I.A. (2004). What is the importance of multivesicular bodies in retrograde axonal transport in vivo? J. Neurobiol. *58*, 230–243.

Whitehurst, A.W., Wilsbacher, J.L., You, Y., Luby-Phelps, K., Moore, M.S., and Cobb, M.H. (2002). ERK2 enters the nucleus by a carrier-independent mechanism. Proc. Natl. Acad. Sci. USA *99*, 7496–7501.

Wilsbacher, J.L., and Cobb, M.H. (2001). Bacterial expression of activated mitogen-activated protein kinases. Methods Enzymol. *332*, 387–400.

Wolf, J.A., Stys, P.K., Lusardi, T., Meaney, D., and Smith, D.H. (2001). Traumatic axonal injury induces calcium influx modulated by tetrodotoxin-sensitive sodium channels. J. Neurosci. *21*, 1923–1930.

Yoo, S., Nguyen, M.P., Fukuda, M., Bittner, G.D., and Fishman, H.M. (2003). Plasmalemmal sealing of transected mammalian neurites is a gradual process mediated by Ca(2+)-regulated proteins. J. Neurosci. Res. *74*, 541–551.

Yoon, M., Moir, R.D., Prahlad, V., and Goldman, R.D. (1998). Motile properties of vimentin intermediate filament networks in living cells. J. Cell Biol. *143*, 147–157.

Ziv, N.E., and Spira, M.E. (1995). Axotomy induces a transient and localized elevation of the free intracellular calcium concentration to the millimolar range. J. Neurophysiol. *74*, 2625–2637.